Electronic Supplementary Information

What determines the performance of lanthanide-based ratiometric nanothermometers

Mochen Jia, Zhen Sun, Mingxuan Zhang, Hanyu Xu and Zuoling Fu*

Coherent Light and Atomic and Molecular Spectroscopy Laboratory, Key Laboratory of Physics and Technology for Advanced Batteries, College of Physics, Jilin University, Changchun 130012, China

Characterization

The crystalline structures of all samples were investigated using X-ray diffraction (XRD) patterns detected by a Bruker D8 Focus diffractometer with Cu Kα radiation. The morphologies were presented via a transmission electron microscope (TEM, JEM-2200FS) and a field emission scanning electron microscope (SEM, Philips XL30). Fourier transform infrared (FT-IR) spectra were recorded by a Bruker TENSOR 27 FT-IR spectrometer. The emission spectra were collected via an Andor SR-500i spectrometer assisted by a SR830 DSP lock-in amplifier and a CCD detector under the excitation of a 980 nm diode laser. The temperature-dependent spectra of samples in powder were obtained by a constant temperature control system equipped with a copper thermocouple (TAP-02, the temperature accuracy: ±0.2 K from 40 to 300 °C.). The temperature-dependent spectra of samples in aqueous solution were acquired by a thermocouple and another constant temperature control system equipped with a cuvette holder (QNW Luma 40, the temperature accuracy: better than ±0.15 °C from 0 to 80 °C). The absorption spectrum was measured with a Shimadzu UV-3101PC scanning spectrophotometer.

Table S1. The fitting parameters of Er^{3+}/Yb^{3+} co-doped different host lattices using eqn (1).

Samples	B	$-\Delta E/k_B$	r^2
$NaYF_4$	9.516±0.242	1132.22±12.280	>0.999
YPO_4	5.612±0.053	1101.61±4.667	>0.999
YVO_4	15.534±0.255	1065.93±8.000	>0.999
CaF_2	5.435±0.169	1093.94±14.720	>0.998
YF_3	4.179±0.062	1059.35±7.076	>0.999
Y_2O_3	10.602±0.271	1156.23±12.743	>0.999
BTO	6.814±0.261	1032.94±18.571	>0.997
LAO	8.741±0.158	1018.50±8.936	>0.999
YAG	4.362±0.169	1138.14±17.929	>0.998

Table S2. The parameters of δT for $NaYF_4$: 2%Er^{3+}, 18%Yb^{3+} nanoparticles at different temperatures (calculated based on the standard deviation).

Temperature (K)	$\frac{\delta LIR}{LIR}$	$\frac{\sigma I_2}{I_2}$ (~525 nm)	$\frac{\sigma I_1}{I_1}$ (~545 nm)
333	1.0%	1.8%	2.0%
393	1.3%	3.8%	3.8%
473	1.1%	7.3%	7.5%

Table S3. The comparison of temperature measurement parameters for Er^{3+}/Yb^{3+} co-doped different host lattices at 333 K.

Samples	S_a (K^{-1})	S_r (% K^{-1})	*LIR*	*δLIR*	*δLIR/LIR* (%)	*σI/I* (%)	*δT* (K)
$NaYF_4$	0.0032	1.02	0.320	0.0033	1.04	0.74	1.0
YPO_4	0.0020	0.99	0.206	0.0026	1.24	0.88	1.2
YVO_4	0.0061	0.96	0.635	0.0081	1.27	0.90	1.3
CaF_2	0.0020	0.99	0.203	0.0027	1.34	0.95	1.4
YF_3	0.0017	0.95	0.174	0.0024	1.36	0.96	1.4
Y_2O_3	0.0034	1.04	0.330	0.0085	2.58	1.82	2.5
BTO	0.0029	0.93	0.307	0.0038	1.24	0.88	1.3
LAO	0.0038	0.92	0.411	0.0056	1.36	0.96	1.5
YAG	0.0015	1.03	0.143	0.0033	2.28	1.61	2.2

Table S4. The fitting parameters of YAG: xTm^{3+}, yHo^{3+}, $5\%Yb^{3+}$nanoparticles using eqn (2).

Samples	*a*	*b*	*c*	r^2
x=0.1%, y=0.1%	1.442±0.038	64.20±17.729	−0.012±0.001	>0.992
x=1.0%, y=0.1%	0.345±0.008	22.42±5.427	−0.013±0.001	>0.994

Table S5. The comparison of temperature measurement parameters for YAG: 0.1%Tm^{3+}, 0.1%Ho^{3+}, 5%Yb^{3+} (sample 1) and YAG: 1%Tm^{3+}, 0.1%Ho^{3+}, 5%Yb^{3+} (sample 2) nanoparticles at 333 K.

Samples	S_a (K^{-1})	S_r (% K^{-1})	*LIR*	*δLIR*	*δLIR/LIR* (%)	*σI/I* (%)	*δT* (K)
1	0.0149	0.55	2.717	0.0865	3.18	2.25	5.8
2	0.0043	0.63	0.695	0.0277	3.99	2.82	6.4

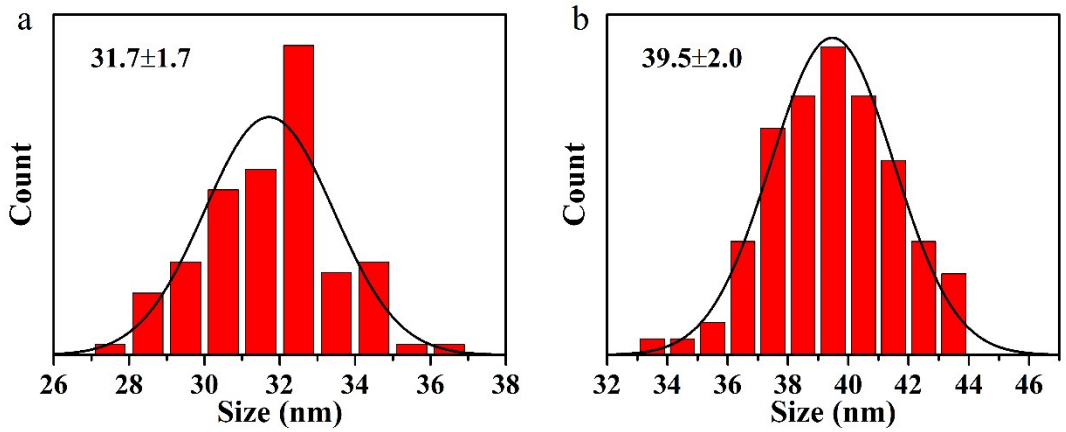

Fig. S1. The TEM-based size distribution histograms of (a) $NaYF_4$: 2%Er^{3+}, 18%Yb^{3+} and (b) $NaYF_4$: 2%Er^{3+}, 18%Yb^{3+}@$NaYF_4$ nanoparticles.

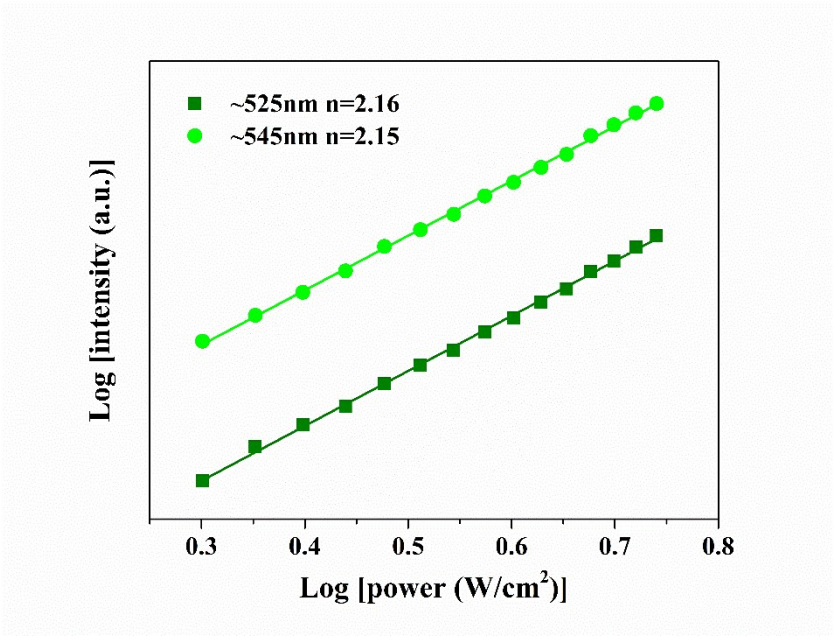

Fig. S2. The power-dependent slope factors (n, $I \sim P^n$) for the ~525 nm and ~545 nm emissions of $NaYF_4$: 2%Er^{3+}, 18%Yb^{3+} nanoparticles. n is the required pump photons of corresponding transition, that is, the slope value in Figure S2. I denotes the corresponding emission intensity, and P represents the excitation power.

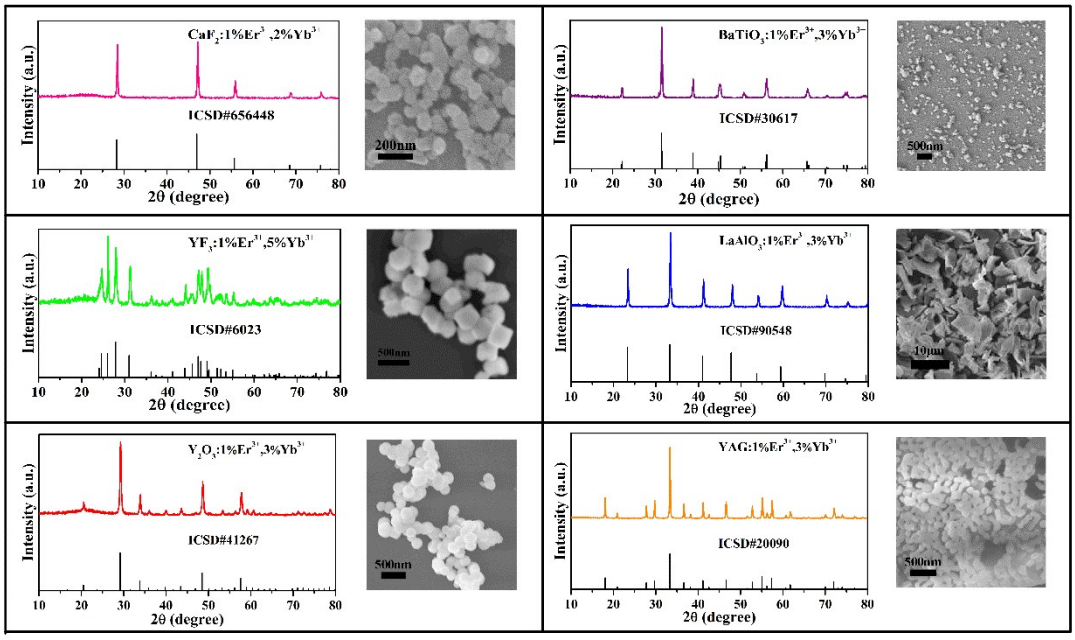

Fig. S3. The XRD patterns and SEM micrographs of Er^{3+}/Yb^{3+} co-doped CaF_2, YF_3, Y_2O_3, BTO, LAO and YAG samples.

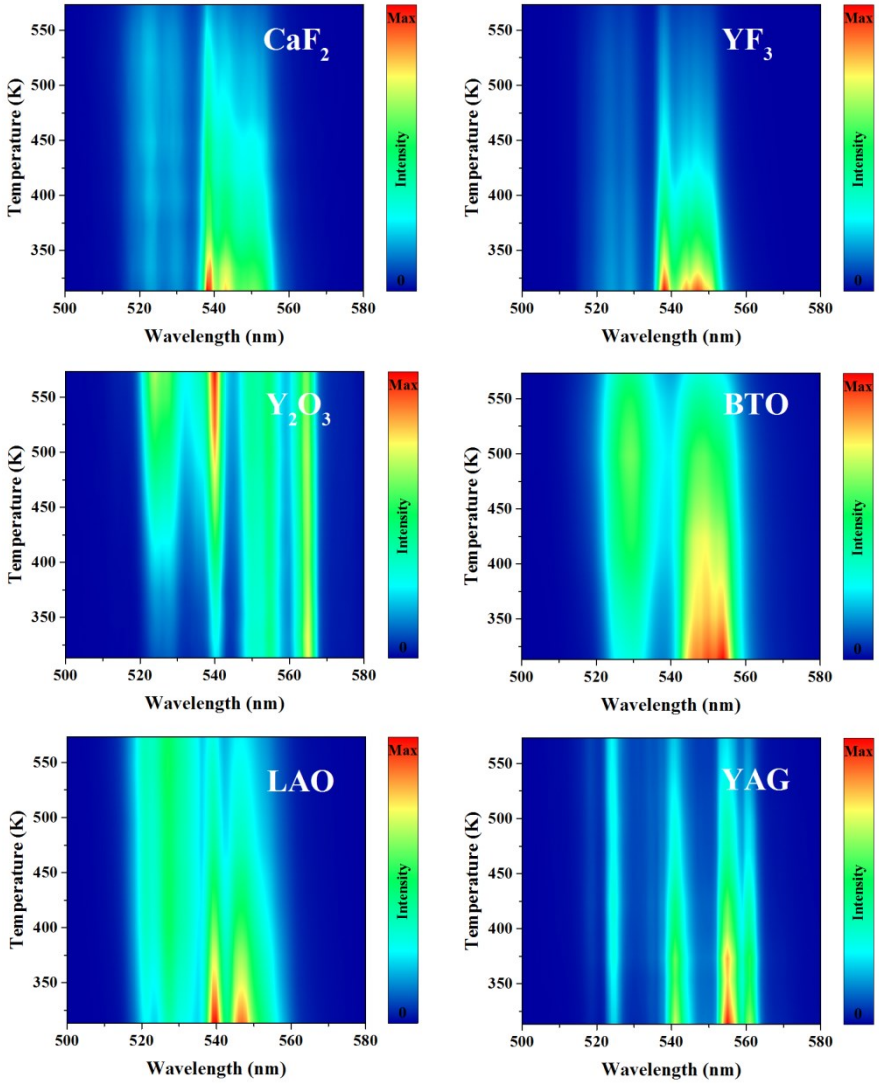

Fig. S4. The contour projections of thermal evolution spectra in 313–573 K range of Er^{3+}/Yb^{3+} co-doped CaF_2, YF_3, Y_2O_3, BTO, LAO and YAG samples.

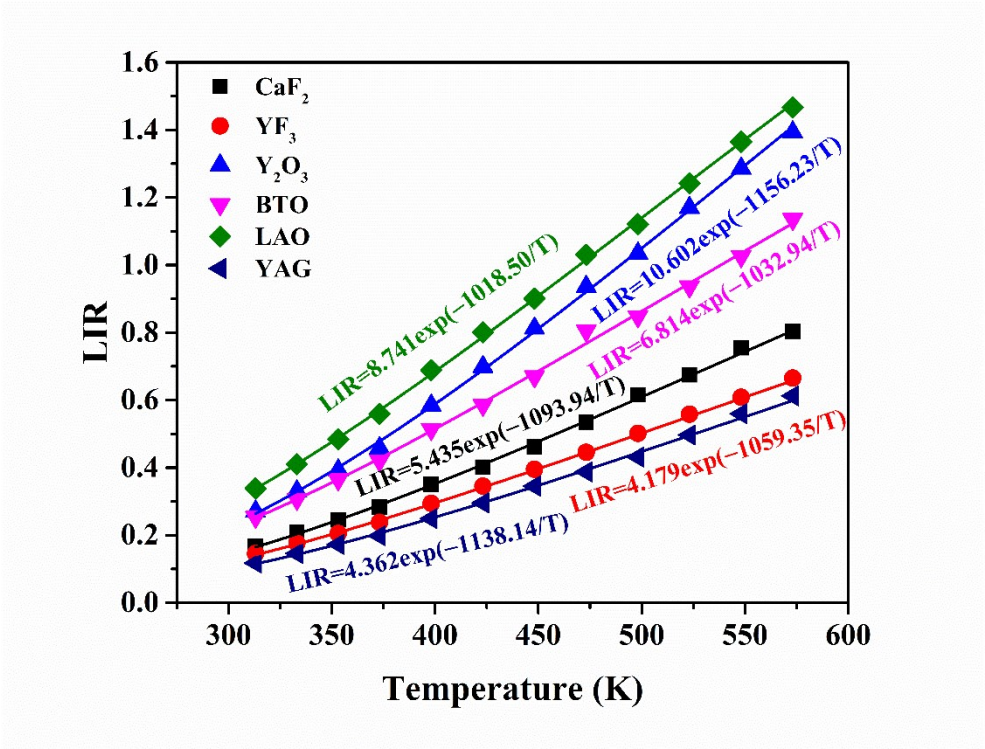

Fig. S5. The calculated calibration curves of Er^{3+}/Yb^{3+} co-doped CaF_2, YF_3, Y_2O_3, BTO, LAO and YAG samples.

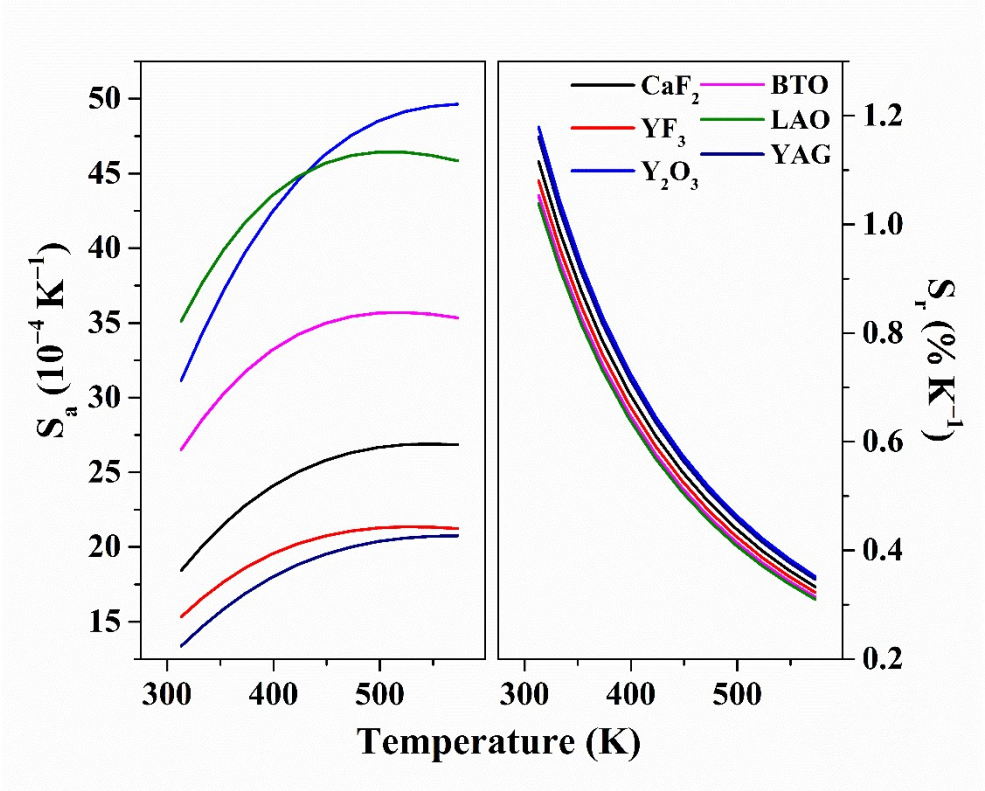

Fig. S6. The S_a and S_r of Er^{3+}/Yb^{3+} co-doped CaF_2, YF_3, Y_2O_3, BTO, LAO and YAG samples.

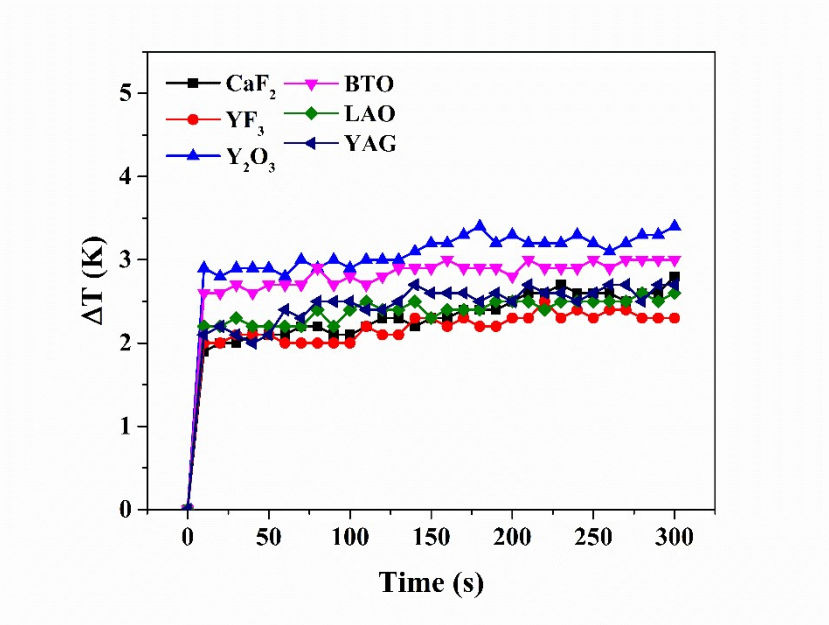

Fig. S7. The elevation of temperature of Er^{3+}/Yb^{3+} co-doped CaF_2, YF_3, Y_2O_3, BTO, LAO and YAG samples under 980 nm excitation with 2.5 W/cm^2.

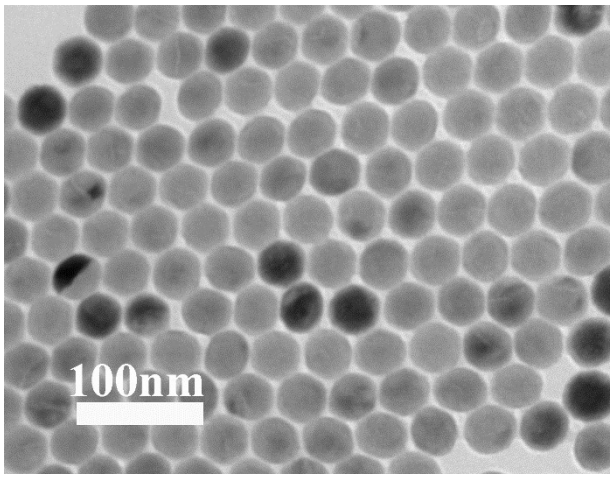

Fig. S8. The TEM image of $NaYF_4$: 2%Er^{3+}, 18%Yb^{3+}@$NaYF_4$ nanoparticles.

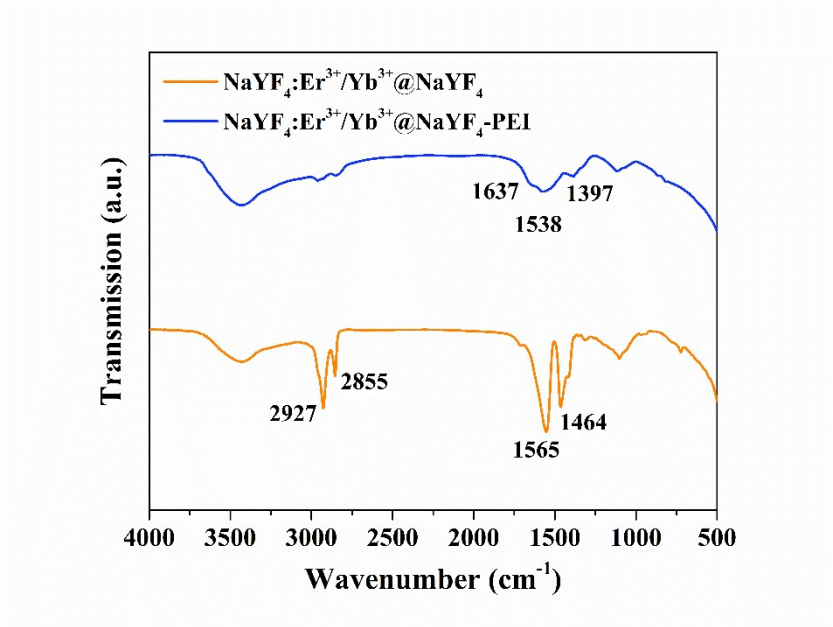

Fig. S9. The FT-IR spectra of OA-capped and PEI-capped $NaYF_4$: 2%Er^{3+}, 18%Yb^{3+}@$NaYF_4$ nanoparticles.

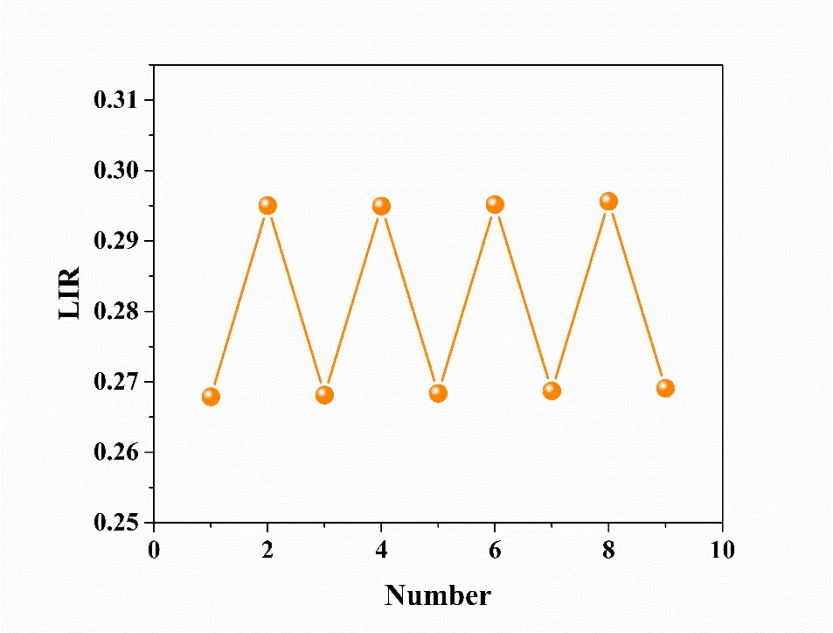

Fig. S10. The temperature-recycle measurements of *LIR* values of $NaYF_4$: 2%Er^{3+}, 18%Yb^{3+}@$NaYF_4$-PEI aqueous solution (500 μg/mL) under 980 nm excitation (2.0 W/cm^2).

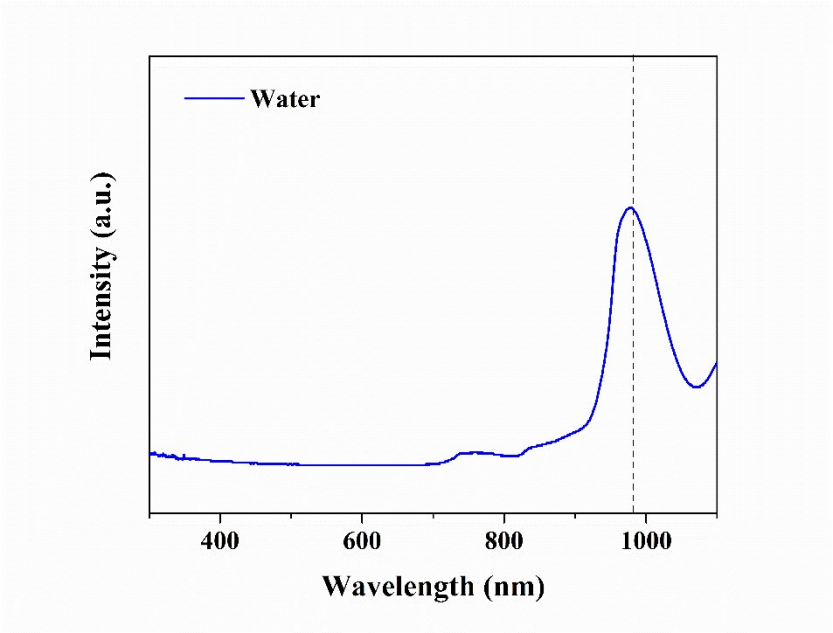

Fig. S11. Overlapping of the absorption spectrum of water and 980 nm excitation.

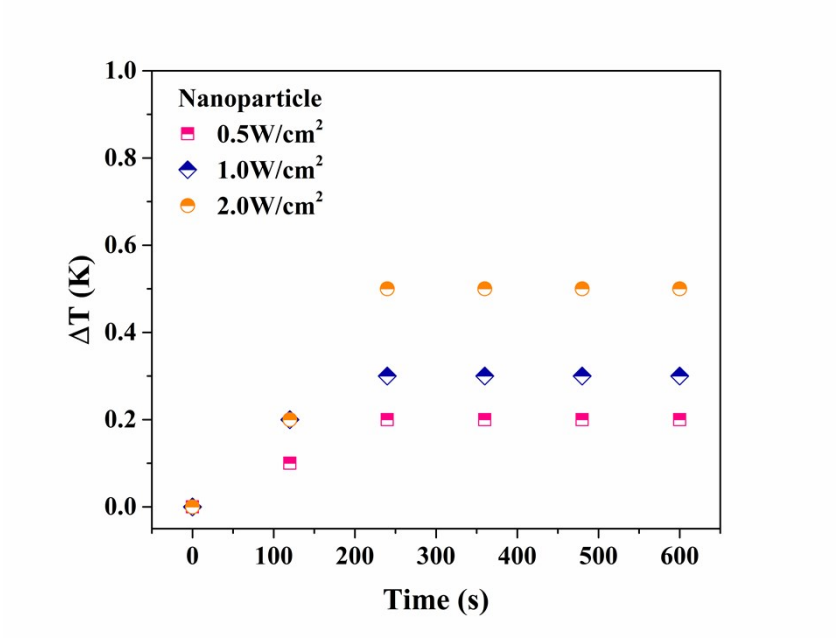

Fig. S12. The time-dependent temperature distributions of $NaYF_4$: 2%Er^{3+}, 18%Yb^{3+}@$NaYF_4$-PEI nanoparticles with different excitation power densities.